Cleaner Materials 15 (2025) 100294

Contents lists available at ScienceDirect

Cleaner Materials

journal homepage: www.journals.elsevier.com/cleaner-materials

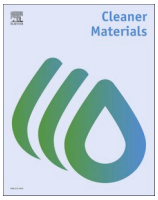

Self-cleaning stone Façades using TiO_2 Microwave-Synthesised Coatings

David Henriques Bento [a], Maria Leonor Matias [a], Maria Magalhães [a], Catarina Quitério [a], Ana Pimentel [a], Dora Sousa [b], Pedro Amaral [b], Carlos Galhano [c], Elvira Fortunato [a], Rodrigo Martins [a,*], Daniela Nunes [a,*]

[a] CENIMAT|i3N, Department of Materials Science, School of Science and Technology, NOVA University Lisbon and CEMOP/UNINOVA, 2829-516 Caparica, Portugal
[b] Instituto de Engenharia Mecânica, Instituto Superior Técnico, Universidade de Lisboa, 1049-001 Lisboa, Portugal
[c] Department of Earth Sciences, School of Science and Technology, NOVA University Lisbon, 2829-516 Caparica, Portugal

ARTICLE INFO

Keywords:
Titanium dioxide nanoparticles
Self-cleaning coatings
Natural stone façades
Microwave synthesis
Photocatalysis
Sustainability

ABSTRACT

This study explores the development and characterization of self-cleaning coatings using titanium dioxide (TiO_2) nanoparticles for natural stone façades, particularly limestone. An energy-efficient, eco-friendly, fast (30 min), and low temperature (110 °C) microwave-assisted solvothermal method is reported for synthesising TiO_2 nanoparticles. These nanoparticles were integrated into coatings that were further applied to limestone substrates via spray-coating, maintaining the stone's appearance while enhancing its self-cleaning properties. Characterization techniques such as X-ray diffraction (XRD), scanning electron microscopy (SEM), scanning transmission electron microscopy (STEM), energy-dispersive X-ray spectroscopy (EDX), UV–VIS spectroscopy and Brunauer-Emmett-Teller (BET) surface area analysis were used to fully characterize the nanopowder. The anatase phase of TiO_2 nanoparticles and a band gap energy of about 3.24 eV were confirmed. SEM and STEM observations revealed that the nanopowder is formed by spherical particles with very fine nanocrystals highly agglomerated, however ensuing a high specific surface area of 199 m^2/g. The self-cleaning properties of the coated limestone were assessed using static contact angle measurements. The results showed a significant enhancement in hydrophilicity, with the static contact angle of the coated limestone substrate reducing to nearly zero even without UV exposure, indicating complete wettability. The coating was also subjected to adhesion tests, confirming the presence of TiO_2 nanoparticles even after multiple cycles. The photocatalytic activity of the developed coating was evaluated using rhodamine B and methyl orange as model pollutants under solar radiation. The coating effectively degraded both model pollutants, and the photocatalytic cycling tests revealed a stable performance after multiple cycles. This research provides a promising approach for creating sustainable and low-maintenance building materials, contributing to preserving natural stone façades and reducing environmental impact in the construction industry.

Introduction

Natural stone is an abundant natural resource used in construction for millenniums due to its natural resistance to environmental conditions. The paradigm changed at the beginning of the 19th century with the Industrial Revolution. Not only did we see an uprising in the use of steel beams and cement, but we also started to observe the consequence of atmospheric pollution on natural stone buildings, especially limestone ones (Snethlage, 2011). However, there are still ways that we can use natural stone in modern construction. Cladding is a technique that consists in using different materials to cover a building's external walls to provide thermal insulation and weather resistance. Using natural stone as cladding offers several environmental benefits. Firstly, natural stones such as granite and limestone can contribute to sustainability by being locally sourced and using traditional construction methods, aligning with principles of sustainable development (Rusu and Muntean, 2022). Additionally, the durability of natural stone cladding plays a crucial role in sustainable construction, as it can lead to longer service life of building components, reducing the need for frequent replacements and associated environmental impacts (Mousavi et al., 2021; Pires et al., 2022). Additionally, natural stone cladding contributes significantly to energy efficiency in buildings due to its low thermal conductivity, which helps in reducing energy consumption for heating and cooling (Spinelli et al., 2019; Anil Kumar, 2015). However, a

* Corresponding authors.
E-mail addresses: rm@uninova.pt (R. Martins), daniela.gomes@fct.unl.pt (D. Nunes).

https://doi.org/10.1016/j.clema.2025.100294
Received 25 October 2024; Received in revised form 7 January 2025; Accepted 8 January 2025
Available online 11 January 2025

common problem in building façades is the accumulation on the surface of inorganic particles and organic compounds that leads to surface darkening (Lettieri et al., 2017), which is visually unpleasant. In the case of cement-covered bricks, there is always the option to remove the paint coating and reapply it. However, for natural stone façades, this is not possible and thus it is necessary to clean them with power tools and chemical detergents. Applying self-cleaning coatings to natural stone façades can reduce energy consumption and minimize the use of chemicals that may harm the environment (Padmanabhan and John, 2020).

Self-cleaning is a natural behavior observed in both animals and plants, enabling them to keep vital body parts free from debris, which enhances their adaptability and survival. In some fish, it is their scales and in some reptiles like geckos, it is their feet. Naturally, humans observed this behavior and sought to replicate this effect on surfaces that need to be constantly clean, for example, solar panels, (Syafiq et al., 2022) or even surfaces that are harder to reach, for example, sky-scrapers' windows (Wu et al., 2023). Self-cleaning surfaces can be achieved by either: superhydrophobicity (Karapanagiotis et al., 2022); superhydrophilicity or photocatalysis (Shaban et al., 2017).

The photocatalytic effect is caused when radiation with an energy greater or equal to the bandgap of a semiconductor material creates an electron-hole pair. This pair can travel to the material's surface, oxidising/reducing water and oxygen molecules. These newly created reactive species react with organic pollutants, transforming them into harmless compounds. As an added effect the surface energy of the material increases, leading to greater hydrophilicity (Schneider et al., 2014).

So, by using photocatalytic materials such as titanium oxide (Padmanabhan and John, 2020; Nunes et al., 2021), zinc oxide (Shaban et al., 2017; Nunes et al., 2021) and other oxides (Rabajczyk et al., 2021; Branquinho et al., 2023) in outdoor applications, where there is sunlight and rain, it is possible to obtain self-cleaning surfaces. The sunlight will provide the ultraviolet radiation needed to cross the bandgap and rain will drag the decomposed pollutants. Since photocatalytic activity also turns the surface of the material superhydrophilic, the rain droplets will spread on the surface covering it entirely, effectively working like a squeegee (Lu et al., 2022; Wu et al., 2023).

Titanium dioxide is a semiconductor material that crystallises in three major structures: rutile, anatase, and brookite (Rao Kandregula et al., 2014). It exhibits a band gap of 3.0 eV, 3.2 eV, and 3.13 to 3.4 eV for each phase respectively (Matias et al., 2023). Both anatase and rutile are used for their enhanced photocatalytic and superhydrophilic behavior (Choi et al., 2024; Nunes et al., 2021; Nunes et al., 2019). However, it is more prominent in anatase due to its surface band bending having a steeper potential and higher surface area than rutile (Padmanabhan and John, 2020). Currently, it is used to produce one of the most used white pigments in the world, titanium white (Gázquez et al., 2021). Due to its wide bandgap, TiO_2 self-cleaning coatings can only be used in outside applications, since the energy to overcome the band gap resides in the ultraviolet radiation (Matias et al., 2023).

Over the years self-cleaning has started to be used in construction materials besides windows, such as cement, where TiO_2 nanoparticles (NP) can be mixed in during the cement's preparation and has achieved promising results (Gryparis et al., 2022). It has been reported previously that TiO_2 NPs were used as self-cleaning coatings for limestone (Calia et al., 2017; Fornasini et al., 2019; Raghavan, 2023). In Ref (Fornasini et al., 2019), TiO_2 NP coatings were developed to create self-cleaning limestone façades. However, they achieved this by applying the coating with a brush, which can compromise the homogeneity of the coating and it is not practical on up-scaling approaches. In another study (Lettieri et al., 2017), researchers developed TiO_2 NP coatings for limestones using sol–gel and a conventional hydrothermal method, which were further deposited by spray-coating. The sol–gel/hydrothermal method resulted in a mixture of rutile and anatase phases, and the substrate's porosity was investigated. However, this study lacks a subsequent analysis of continuous pollutant degradation, which the present work will address.

TiO_2 nanoparticles have been produced by several methods, including sol–gel (Raghavan, 2023); microemulsion technique (Gupta and Tripathi, 2012), precipitation (Wang, et al., 2020), electrochemical processes (Anandgaonker et al., 2019), conventional hydrothermal and solvothermal methods (Gupta et al., 2021; Nam et al., 2013), microwave irradiation (Matias et al., 2023; Matias et al., 2022a; Matias et al., 2022b), among others. The latter has several advantages over these production routes, including fast heating speeds leading to energy-saving, and a uniform heating system, so that it can rapidly prepare nanoparticles with a narrow particle size distribution and uniform morphology (Yang and Park, 2019), besides its high yield (Branquinho et al., 2023). In the present study, microwave irradiation was selected followed by spray coating to deposit these nanoparticles. The deposition method was chosen since it is possible to be used on large surfaces, which means it can be used in both experimental and industry environments, despite its versatility, simplicity, and cost-efficiency (Alanazi, 2023). Additionally, this type of deposition method reduces waste compared to other deposition methods such as dip-coating or *in situ* growth, and creates uniform coatings (Del Secco et al., 2022). Additionally, this technique can minimize the modification of the appearance of the substrates, which is an important aspect of construction.

The present study is intended to be a viable and sustainable way for industry manufacturing of TiO_2 nanoscale coatings for stone façades, without altering the stone's color/aspect. TiO_2 nanoparticles were synthesised via a fast (30 min) and low-temperature (110 °C) solvothermal method assisted by microwave irradiation. The TiO_2 coatings' deposition was further carried out by spray-coating, and its self-cleaning properties were assessed together with its photocatalytic activity efficiency tested with rhodamine B and methyl orange under solar radiation. Additionally, consecutive degradation cycles were performed to test the stability of the nanoparticles.

Materials and methods

Microwave synthesis and spray coating deposition

Stone panels were cut into 20 x 20 x 6 mm pieces with 6 mm of thickness to ease the manipulation of samples. After cutting, the samples were cleaned in ultrasonic baths for 15 min in ultrapure water. They were then dried in a vacuum desiccator for one day until the mass of the stone samples was constant.

TiO_2 nanoparticles were prepared by mixing 1 mL of titanium butoxide ($Ti(OBu)_4$) in 12 mL of isopropanol alcohol (IPA) and 0.625 mL of hydrochloric acid. The solution was mixed until homogeneous and transferred to a microwave vessel for synthesis. The solution was heated in a microwave synthesizer – CEM Discover SP for 30 min at 110 °C and 115 W. After that, the vesseĺs content was centrifuged at 5200 rpm and washed in IPA several times. The precipitate was left to dry overnight in a desiccator at 60 °C. The TiO_2 NPs were collected in powder form.

For the spray-coating ink formulation, the TiO_2 NPs in powder form were dissolved in ethanol to achieve a concentration of 0.1 % w/v with the help of an ultrasonic bath until the solution was homogeneous. Polyacrylic acid (M_W = 2000) was added to the solution with a mass ratio of 1:10 relative to the TiO_2 NPs. Each formulation of ink was prepared before deposition.

The TiO_2 nanoparticles' inks were spray-coated directly onto the 20 x 20 x 6 mm limestone substrates. The samples were pre-heated at 120 °C, and sprayed at a 10 cm distance, with a pressure of 1 bar, for 0.4 s for each layer. 30 layers were deposited in each sample. Between each layer, there was a waiting time of 1 min to ensure the solvent of the ink evaporated.

Structural and optical characterization

X-ray diffraction patterns were collected using a PANalytical Aeris benchtop X-ray diffractometer (Malvern) equipped with a Cu Kα source operating at 40 kV and 15 mA. Data were collected in the 2θ range 10–90° with a step interval of 0.05°. The simulated TiO_2 anatase phase was indexed using the International Centre for Diffraction Data (ICDD) file No. 021–1272.

The specific surface area was estimated by nitrogen adsorption according to the BET method, which was applied in the p/p0 range determined following the Rouquerol criteria (Rouquerol et al., 2007). The data were obtained at 77 K in the adsorption apparatus (Autosorb IQ, Quantachrome). Before the experiments, the TiO_2 nanopowders (~0.2 g) were outgassed overnight at 120 °C, under a vacuum better than 10^{-2} Pa.

SEM images were acquired using a Hitachi Regulus 8220 Scanning Electron Microscope, which was equipped with an EDX detector from Oxford Instruments.

Scanning Transmission Electron Microscopy (STEM) observations, along with High-Angle Annular Dark-Field (HAADF) imaging, were conducted using a Hitachi HF5000 field-emission transmission electron microscope, operating at 200 kV. This instrument is a probe-corrected cold FEG (Field Emission Gun) equipped with a 100 mm^2 EDX detector also from Oxford Instruments. A drop of the sonicated dispersion was applied to lacey-carbon copper grids and left to dry before observation. The average particle size and standard deviation of the TiO_2 structures were determined by analysing the dimensions of 30 nanoparticles based on STEM data (Schneider et al., 2012).

Total reflectance and absorbance measurements were recorded using a UV–VIS-NIR Perkin Elmer's Lambda 950 spectrophotometer with an integrating sphere in the 200–800 nm range. The specular reflectance was also recorded in the same range to obtain the diffuse reflectance data (DRS) and estimate the band gap energies (E_g). A Spectralon® (Labsphere, United Kingdom) was used as the reference. Measurements were carried out at room temperature (RT). Due to titanium oxide's indirect band gap and the sample's thickness the Kubelka-Munk method was used to estimate the energy band gap (Makuła et al., 2018).

Static contact angle measurements were performed on the 20 x 20 x 6 mm substrates using an OCA 15 plus (Dataphysics, Germany) through a sessile drop method. The results of nine measurements at different points were averaged to determine the mean and the standard deviation.

The adhesion of the transparent TiO_2 coating on limestone was evaluated considering a tape adhesion test adapted for this specific application. Since the coating is transparent and not a dense film, the standard ASTM D3359 (ASTM International, 2023) method involving cuts was deemed non-applicable. Instead, the coated surface underwent 10 cycles of tape application (direct adhesive contact) and removal (peel-off). Following this test, SEM imaging and EDX analyses were performed to evaluate morphological changes and confirm the presence of TiO_2.

The coating's thickness measurements were performed using an XP-Plus Stylus Profiler from Ambios Technology, USA, equipped with a 2 μm radius stylus. The 1500 μm scans were performed with a nominal force of 10 mg. Profilometry measurements were performed on a half-coated, half-pristine limestone stone to determine the thickness of the coating. The profilometer measurements were also performed on half-pristine and half-coated glass substrates due to the natural rough aspect of the limestone samples that could hinder the acquisition of the coating's thickness.

Photocatalytic experiments

Rhodamine B (RhB) and methyl orange (MO) with concentrations of 0.05 g/dm^3 and 0.5 g/dm^3, respectively, were deposited on the surface of 20 x 20 x 6 mm substrates via spray coating. A higher concentration of MO was chosen to increase the color contrast. The substrates were sprayed at a 10 cm distance, at 1 bar of pressure, for 0.4 s for each layer and with 10 layers. Between each layer's deposition, there was a waiting time of 2 min to ensure the solvent of the contaminants evaporated and avoid coffee ring effects.

The degradation of pollutants was studied under an LS-2 LED Lamp Solar Simulator (WAVELABS, Germany) with AM 1.5 spectrum, at an intensity of 1000 W/m^2. The color was monitored using a WR10-8 colorimeter (FRU, China). Three measurements were carried out on each sample. Color characteristics were referred to in the CIE*Lab* space, which expresses colors through the parameters L^*, a^*, and b^*, representing brightness and the red/green and yellow/blue chromatic intensities, respectively. The aspect change after coating the limestone façades was quantified through ΔE, which is calculated using Equation (1) (Lettieri et al., 2019; Mokrzycki and Tatol, 2011).

$$\Delta E = \sqrt{(\Delta L^*)^2 + (\Delta a^*)^2 + (\Delta b^*)^2} \quad (1)$$

For RhB degradation tests, the parameter a^* was chosen to study the color change, while parameter b^* was selected for MO degradation tests. Degradation values (D%) were obtained following Equation (2) and (3) (Lettieri et al., 2019):

$$D_a\% = \left|\frac{a_0^* - a_t^*}{a_0^* - a_c^*}\right| \times 100 \quad (2)$$

$$D_b\% = \left|\frac{b_0^* - b_t^*}{b_0^* - b_c^*}\right| \times 100 \quad (3)$$

Where a_0^* is the initial a^* value where the contaminant is at its maximum, a_t^* is the a^* value after t minutes of irradiation and a_c^* is the a^* value of the clean stone. The same applies for D_b%.

Results and discussion

TiO_2 nanopowder characterisation

The crystalline structure of the microwave synthesised TiO_2 nanoparticles was studied by X-ray diffraction, and the obtained diffractogram can be seen in Fig. 1. A highly crystalline powder is observed, and by comparing the simulated XRD diffractogram, it can be concluded that the experimental XRD diffractogram corresponds entirely to the anatase TiO_2 phase. Additionally, it is also possible to verify the absence of impurities. From XRD measurements, it could be inferred that just 30 min is sufficient to fully crystallize anatase nanomaterials at a low

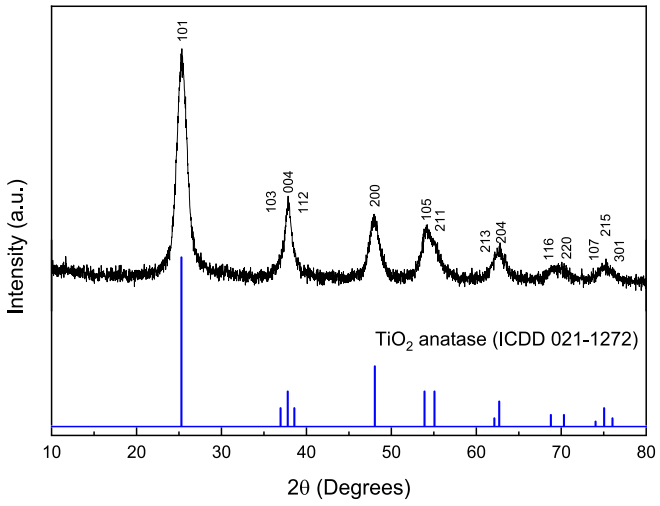

Fig. 1. XRD diffractogram of the synthesised TiO_2 nanopowder together with the simulated anatase XRD pattern.

synthesis temperature (110 °C).

Fig. 2 depicts the SEM images of the TiO_2 nanomaterials synthesised under microwave irradiation, revealing the formation of large and compact aggregates of TiO_2 nanocrystals with a spherical shape. These aggregates exhibited sizes ranging within 650 ± 210 nm (Fig. 2 (a)). The EDX analyses were carried out simultaneously in the same area of the SEM image (Fig. 2 (a)), and confirmed the lack of impurities, detecting only Ti and O on the TiO_2 aggregates. The EDX spectrum from 0-10 keV can be found in Supplementary Information Figure S 1, which further confirms the lack of impurities.

Further investigation of the TiO_2 nanomaterial was conducted using scanning transmission electron microscopy, revealing the formation of large aggregates primarily assuming a spherical shape, although elongated structures were also observed (Fig. 3 (a)). Analysis of Fig. 3 (b) and its inset indicated that these larger aggregates consist of very fine nanocrystals, featuring both curved and faceted edges. Additionally, these aggregates displayed a high level of compactness while exhibiting nanoscale porosity, as indicated by arrows in Fig. 3 (b). The average size of TiO_2 nanocrystals was determined to be 4.23 ± 0.66 nm.

The nanocrystals were observed using HAADF imaging (Fig. 3 (c) and (d)), and the contouring of the nanocrystals was performed to illustrate their close packaging, with markings indicating the locations where fast Fourier transform (FFT) patterns were obtained.

HAADF images depicted Ti atom columns, with a measured lattice spacing of 0.38 nm, corresponding precisely to the (1 0 0) and (0 1 0) atomic planes of anatase. Observed along the [001] zone axis, the angles between (1 0 0) and (0 1 0) were observed to be 90°, consistent with the theoretical value reported for pure crystalline TiO_2 anatase (ICDD 021–1272).

UV–VIS spectroscopy was performed to determine the energy band gap of the synthesised TiO_2 NPs. The Kubelka-Munk method was used to estimate the energy band gap, which sits around 3.24 eV, which is in good agreement with the literature data for anatase band gap (Matias et al., 2023; Wu et al., 2023).

The Brunauer-Emmett-Teller (BET) analysis was performed to determine the specific surface area of the TiO_2 NP powder. BET-specific surface area was measured to be 199 m^2/g, with an average pore size of 4.4 nm. The high specific surface area value is in line with similar studies for anatase nanoparticles (Brišević et al., 2024; Drunka et al., 2016; Suwarnkar et al., 2014; Sanchez Tobon et al., 2022), however, considering lower microwave synthesis temperatures for the present study. Thus, this high surface area measured is expected to boost the pollutant adsorption capacity and provide more active sites for photocatalytic reactions, enhancing the overall photocatalytic performance of the system (Amano et al., 2010). The TiO_2 NP powder exhibits a Type IV isotherm (Supplementary Information Figure S 2) according to the IUPAC classification, indicating mesoporous characteristics. Type IV isotherms are typically associated with mesoporous materials, which have pore diameters between 2 nm and 50 nm. These isotherms are characterized by an initial region resembling a Type II isotherm, followed by a hysteresis loop due to capillary condensation within the mesopores (Thommes et al., 2015).

TiO_2 coating characterisation

To fully characterize the pristine substrates, SEM and EDX analyses were performed on uncoated limestone façade substrates (Fig. 5)). From Fig. 5.b-e, it is possible to observe the presence of C, O and Ca, which is expected since limestone is made of different crystalline forms of calcium carbonate ($CaCO_3$). Mg is also present in the sample as it can naturally occur in small amounts in limestone, either in the form of magnesium oxide (MgO) or magnesium carbonate ($MgCO_3$) (Silva, 2022; Rodrigues, 2019).

The substrates were also investigated after deposition (Fig. 6). The spray-coating was successfully used to deposit the TiO_2 coatings since the SEM image (Fig. 6a) shows that the TiO_2 particles are uniformly deposited and well dispersed. Additionally, through EDX, it can be seen the elements coming from the substrate, but also Ti from the deposited coating. No impurities were detected that could compromise the effectiveness of self-cleaning. Compared to similar studies in the literature, it can be concluded that the approach developed in this study results in more coverage of the stone surface with a more uniform dispersion (Lettieri et al., 2017; Gryparis et al., 2022; Quagliarini et al., 2012). Profilometer measurements were used to infer the thickness of the TiO_2 coating. The profilometer results (Figure S 3) show a coating thickness of approximately 1.19 μm on the glass substrate, where a clear step can be seen in the transition from pristine glass to coated glass (Figure S 3a). Additionally, the arithmetic average roughness (Ra) of the coating on the glass substrate was calculated to be 0.36 μm. Regarding the coating thickness on the limestone, it is impossible to determine, since no step

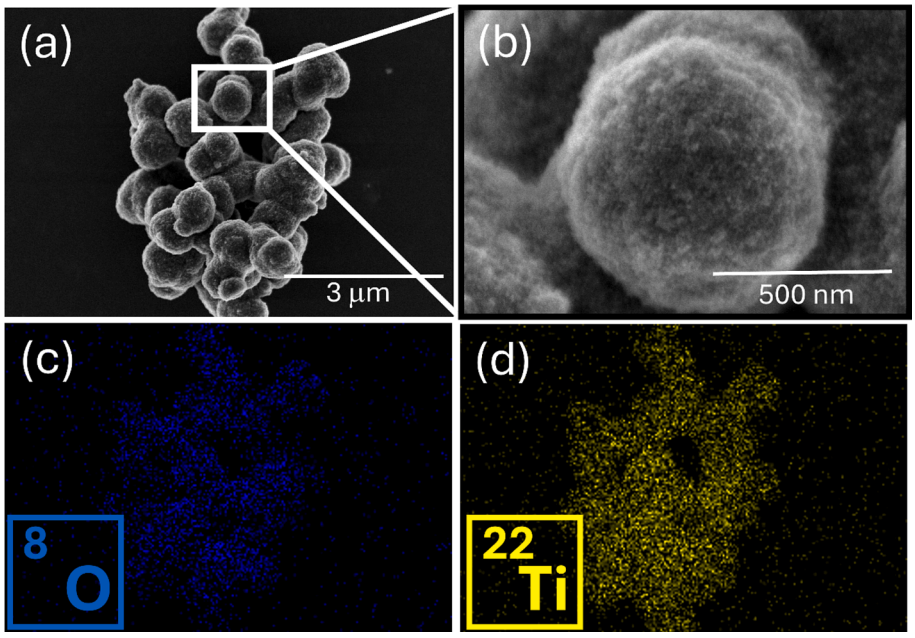

Fig. 2. SEM images of the TiO_2 nanostructures (a and b), together with the EDX maps of O (c) and Ti (d).

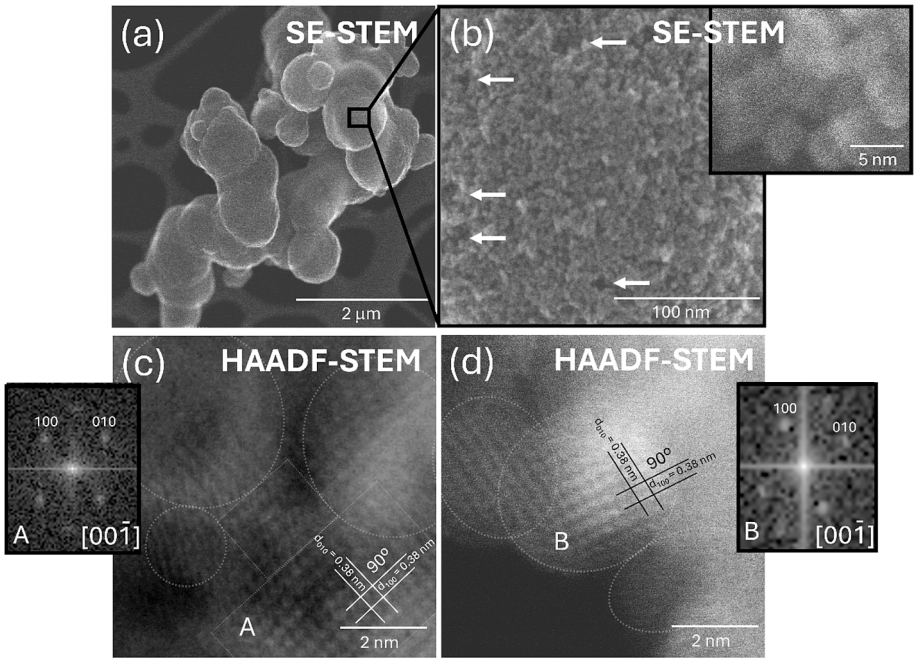

Fig. 3. (a) and (b) SE-STEM images of the TiO_2 aggregates highlight their porous (see arrows) and compact characteristics. The inset shows that the aggregates are composed of very fine nanocrystals. (c) and (d) HAADF-STEM images of the TiO_2 nanocrystals with the corresponding FFT images carried out at the nanocrystals indicated as A and B.

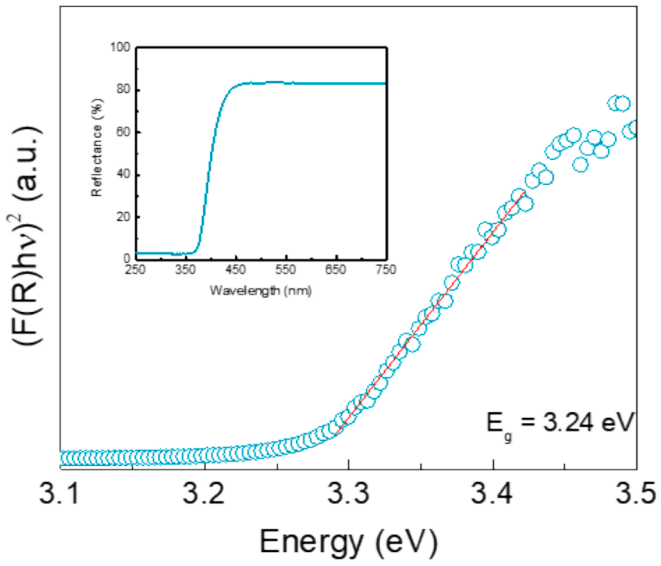

Fig. 4. Kubelka-Munk reflectance spectrum and energy band gap of the TiO_2 nanopowder. The inset shows the RT reflectance spectrum.

can be seen in the profile (Figure S 3b). This is due to the natural roughness of limestone substrates being greater than the roughness of the coating. The Ra of the pristine limestone substrate was determined to be 6.05 µm. Regarding the coated limestone substrate, the Ra was determined to be 4.14 µm, which means that the coating decreases the Ra of the surface of the limestone. As for the root mean square roughness (Rq), the values are 7.67 µm and 4.87 µm, for pristine and coated limestone, respectively.

Adhesion tests were carried out on the coated limestone substrate. The tape adhesion test revealed some coating detachment; however, a substantial presence of TiO_2 particles was still observed after 10 peel-off adhesion cycles. In fact, EDX confirms the presence of Ti and O elements, indicating that the coating resisted the tape adhesion test. This acceptable stability of the coating can be attributed to the interaction between the polyacrylic acid binder and the limestone surface, enhancing the adhesion. The EDX mapping results after adhesion tests are presented in the Supplementary Information Figure S4.

Using a colorimeter it is possible to ascertain that the coating didn't significantly change the aspect of the stone. The individual value changes for each parameter can be seen in Table 1, with the global color change as well. It has been reported that for values of ΔE lower than 1, an observer cannot notice the difference between the substrates (Mokrzycki and Tatol, 2011).

Static contact angle

One of the key aspects of self-cleaning is the ability to use rainwater to wash away debris that ends up on the surface. This can be achieved by creating a super hydrophilic surface that makes water behave like a squeegee (Lu et al., 2022; Wu et al., 2023). TiO_2 NPs possess a high concentration of hydroxyl groups on their surface (Barilyuk et al., 2024), which means that when deposited onto the limestone façades it will increase the interaction between the surface and water. Static contact angle (SCA) measurements were performed in uncoated and coated limestone substrates to determine their wettability. Fig. 7 (a) shows that uncoated limestone substrates possess an average SCA of (38 ± 8)°. In Fig. 7 (b), the total wettability (SCA < 5°) of the stone surface can be observed on TiO_2-coated substrates. Whereas in other studies (Bergamonti et al., 2016; Lettieri et al., 2017; Fornasini et al., 2019) the superhydrophilicity is only attained after irradiance with UV light, the developed coating presents the same characteristic without exposure to a light source. Few studies describe the superhydrophilicity of TiO_2 coatings without plasma or UV treatments (Zorba et al., 2010; Hosono et al., 2007; Wang et al., 2011; Fujishima and Zhang, 2006). When the TiO_2 film is irradiated by UV light, a photo-induced redox reaction produces active oxygen on the film surface, and the UV irradiation creates surface oxygen defects on the TiO_2 surface, enhancing the surface's suitability for the dissociative adsorption of water, resulting in superhydrophilicity (Wang et al., 2011; Fujishima and Zhang, 2006). Other approaches to increase the hydrophilicity of TiO_2 coatings have

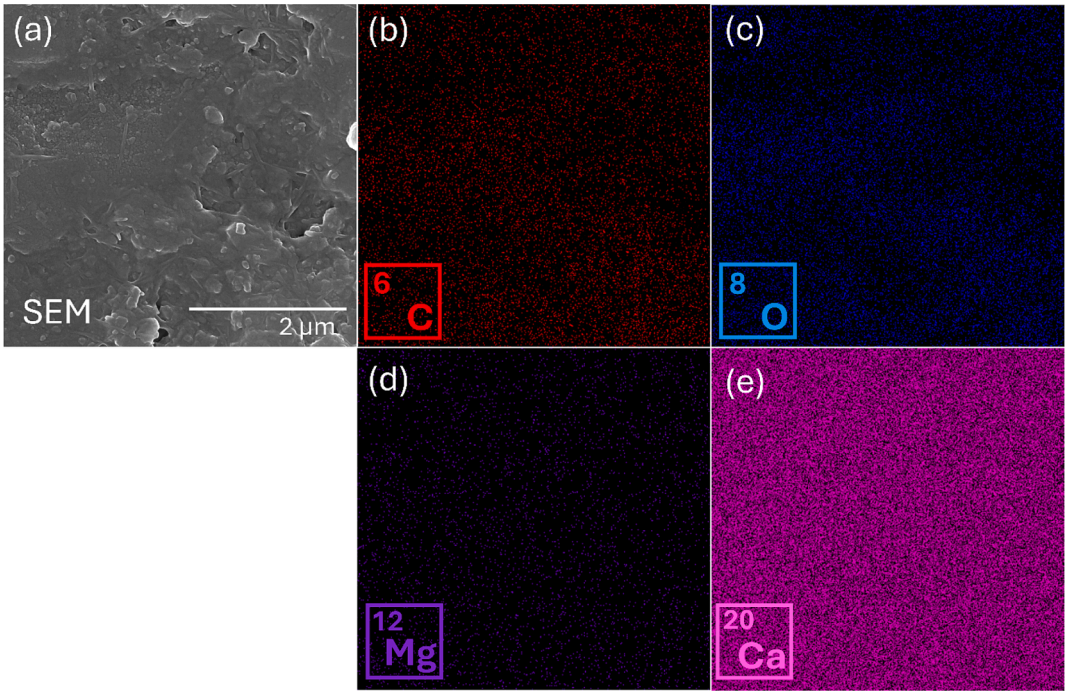

Fig. 5. (a) Representative SEM image of uncoated limestone façade, with EDX maps of (b) carbon, (c) oxygen, (d) magnesium and (e) calcium.

also been reported, including engineering surface morphology. For instance, increasing surface roughness can make the surfaces of hydrophilic materials more wettable, especially for porous coatings (Wang et al., 2011). Moreover, it is also known that nanoscale roughness affects surface wetting (Kameya and Yabe, 2019). Zorba et al. (Zorba et al., 2010) reported a TiO_2 coating composed of ~ 200 nm aggregates, in which the superhydrophilic surface of the film without exposure to UV irradiation was attributed to the intrinsic hydrophilic property of TiO_2 combined with a hierarchical porous nanostructure of the coating. In the present study, the superhydrophilicity observed is expected to have contributions from the structure of the developed coating at both nano and micrometer ranges. The microwave-synthesised TiO_2 aggregates exhibited nano-porosity (Fig. 3) and high surface area (199 m^2/g), which leads to higher hydrophilicity at the nanoscale (Bolis et al., 2012). Moreover, these aggregates modify the pristine stone surface, forming a nanostructured coating with a thickness of ~ 1.2 µm (see profile in Figure S3), increasing surface roughness at the nano and micrometer scales. From a macroscale perspective, the overall surface roughness is reduced by the filling of stone orifices with the TiO_2 coating (the average roughness of the pristine stone was measured at 6.05 µm, in contrast to 4.14 µm for the coated stone substrate). Associated with this multiscale wettability effect, the PAA polymer can also contribute to the increase in hydrophilicity observed due to its natural hydrophilic character (Zhou et al., 2021). Nevertheless, the superhydrophilic behavior of the developed coating is expected to be a synergetic effect of the nano/micro-structures at the surface and intrinsic properties of the nanomaterial (Mittal, 2022; Padmanabhan and John, 2020).

RhB and MO photocatalytic tests

The photocatalytic activity of coated substrates was evaluated to assess the self-cleaning properties of the approach presented in this study. The photo-degradation of RhB and MO under simulated solar radiation was used to determine the photocatalytic activity of the coated substrates (as shown in Figure S 5 and Figure S 6). RhB and MO degradation tests (Fig. 8a) show that after 8 h of exposure, the TiO_2 coating degrades 85 % of the total RhB and 60 % of the total MO present in the surface. The uncoated limestone façade substrates reached degradation values of approximately 60 % for RhB and 50 % for MO. The degradation of MO appears to be lower when compared to RhB, however, this is expected since MO was in higher concentration than RhB. The difference in concentrations is due to low contrast in MO-polluted substrates. Since the degradation of pollutants is measured by comparing CIE*Lab* values, a higher concentration of MO was needed to create a color difference. When compared to the uncoated substrates, it is clear that the coating's photo-degradation of both pollutants is expressively higher under solar radiation. Nevertheless, a considerable degradation contribution coming from the uncoated substrate is expected, in accordance to previous studies (Quagliarini et al., 2012; Lettieri et al., 2019). It is known at least for RhB that its degradation under light exposure occurs to some extent, even in absence of self-cleaning coatings (Lettieri et al., 2019). Moreover, the presence of other oxides in the substrate surface, i.e., MgO could contribute to the photocatalytic effect observed with uncoated substrates (Balakrishnan et al., 2020). Nevertheless, among the few studies in literature, most of them use UV light as the light source (Lettieri et al., 2019) and just consider one pollutant to determine the photocatalytic activity, without investigating the stability during consecutive cycles (Bergamonti et al., 2016; Lettieri et al., 2017; Fornasini et al., 2019).

In terms of the structure of the TiO_2 nanoparticles and the overall photocatalytic performance in the presence of both model pollutants, it is known that numerous factors influence the photocatalytic behavior of TiO_2, including its crystalline phase, specific surface area, active facets, and particle size (Matias et al., 2023; Guo et al., 2014). Under microwave irradiation, only the anatase phase was obtained (Fig. 1 and Fig. 3), with a band gap value consistent with previous experimental values for anatase (Fig. 4). Despite the controversy over which TiO_2 crystalline phase has higher photocatalytic activity under visible/solar radiation, many studies agree that anatase is considered the most photoactive phase (Matias et al., 2023; Matias et al., 2022b; Luttrell et al., 2015; Zhang et al., 2014). This is due to its slower charge carrier recombination due to the lightest average effective mass of photogenerated electrons and holes, resulting in the lowest recombination rate of charge carriers (Žerjav et al., 2022), and due to the fact that anatase has an indirect band gap, which leads to a longer lifetime of

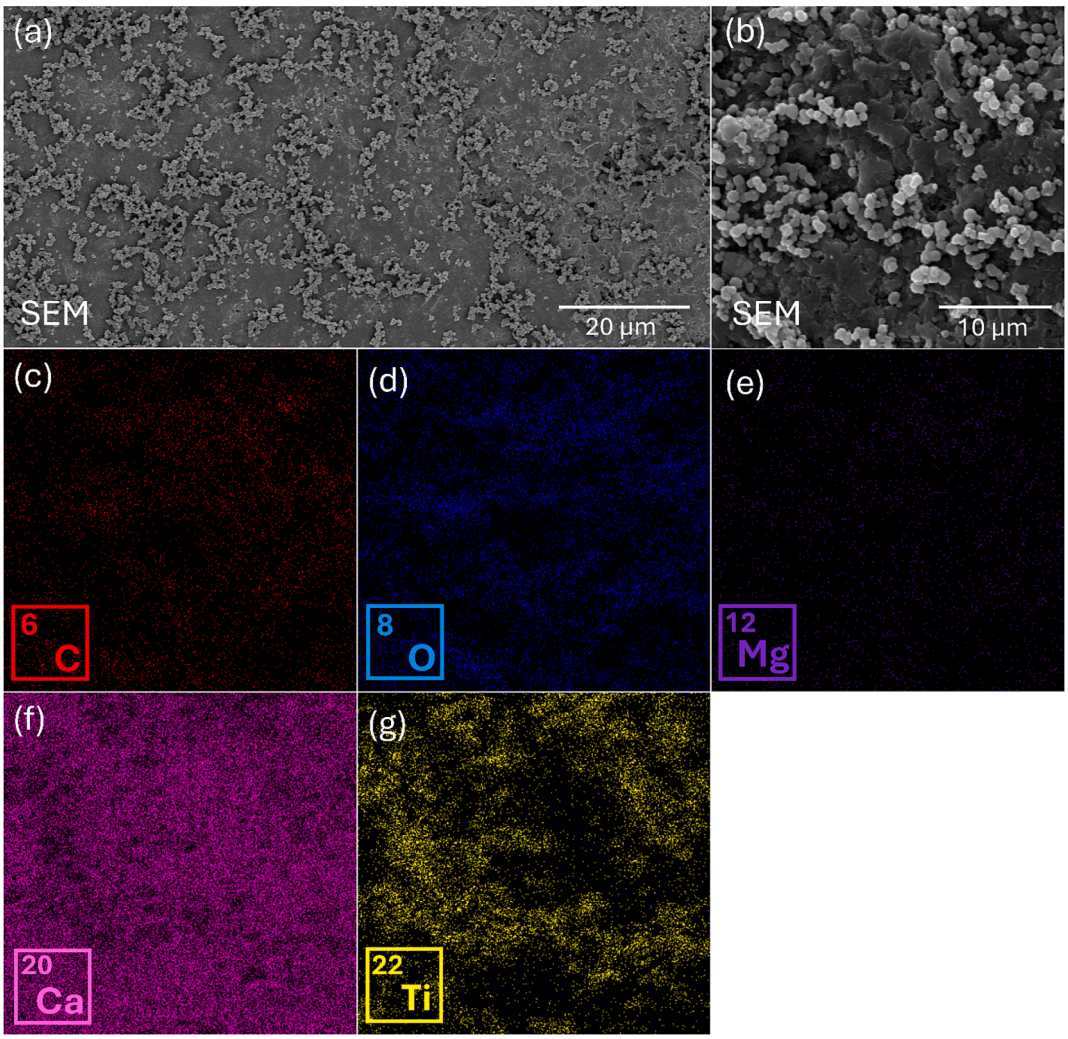

Fig. 6. (a) Representative SEM image of TiO_2 –coated limestone substrate, (b) SEM image of the area considered for the EDX measurements, with the corresponding EDX maps of (c) carbon, (d) oxygen, (e) magnesium, (f) calcium and (g) titanium.

Table 1
Mean values of the changes in the color parameters (ΔL^*, Δa^*, Δb^*) and the global color changes (ΔE) upon coating the substrate.

ΔL^*	Δa^*	Δb^*	ΔE
0.39	0.21	0.58	0.77

photoexcited electrons and holes, and facilitates charge carriers to participate in surface reactions (Matias et al., 2023; Luttrell et al., 2015; Žerjav et al., 2022). In terms of specific surface area, microwave synthesis resulted in a high surface area mesoporous nanopowder, which is expected to deeply impact the photocatalytic performance, as by increasing the surface area, more active surface sites become available, enhancing the production of radical species and pollutant molecule adsorption, and thus increasing the photocatalytic activity (Nunes et al., 2021; Wei et al., 2013). This high surface area is related to the structure of the nanomaterial, and from SEM and STEM analyses, it can be concluded that the TiO_2 aggregates (650 ± 210 nm) are composed of nanocrystals (4.23 ± 0.66 nm), with nanoporosity within the aggregates. The smaller size of the nanocrystals associated with the nanoporosity can provide more active sites for photocatalytic reactions. As a result, the uniform coverage of the substrates and the high specific surface area of the TiO_2 nanoparticles effectively contributed to the

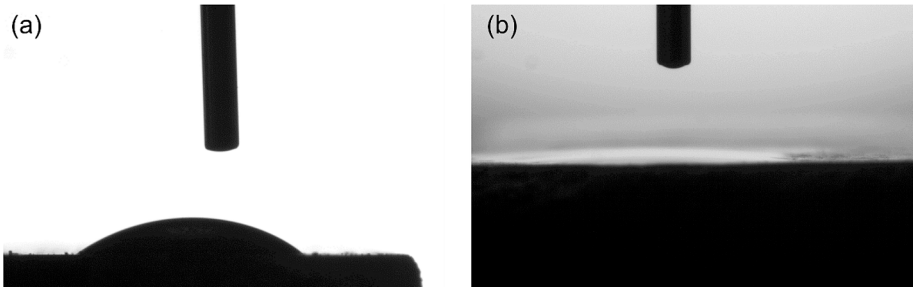

Fig. 7. Static contact angle of (a) uncoated limestone façade and (b) coated limestone façade.

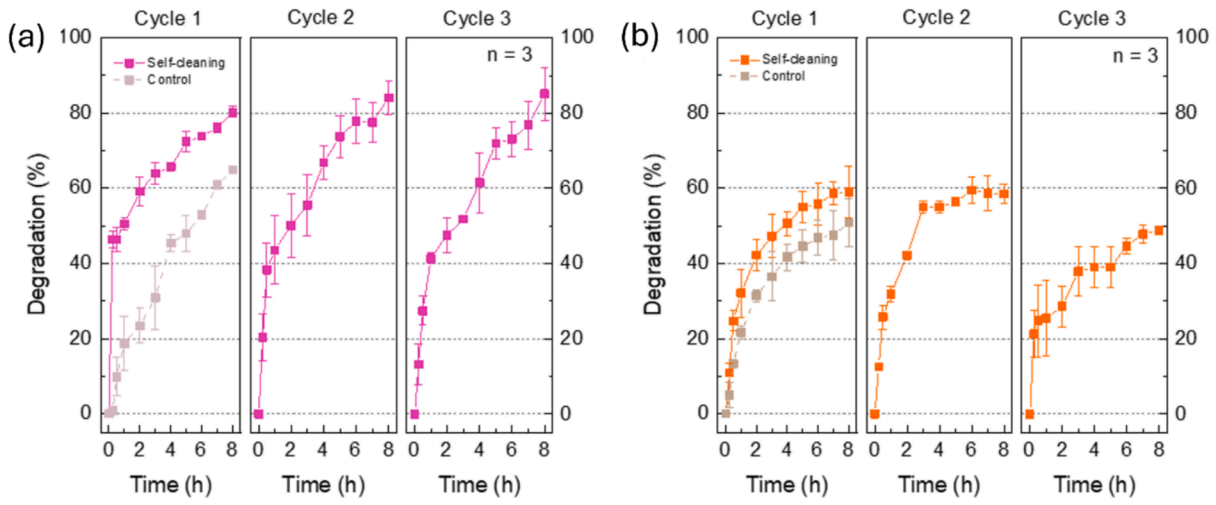

Fig. 8. Cycling of the photocatalytic degradation of (a) rhodamine B and (b) methyl orange in limestone coated with self-cleaning. The degradation was extrapolated from the a* value for rhodamine B and the b* for methyl orange of the CIELab color space. (For interpretation of the references to color in this figure legend, the reader is referred to the web version of this article.). (For interpretation of the references to color in this figure legend, the reader is referred to the web version of this article.)

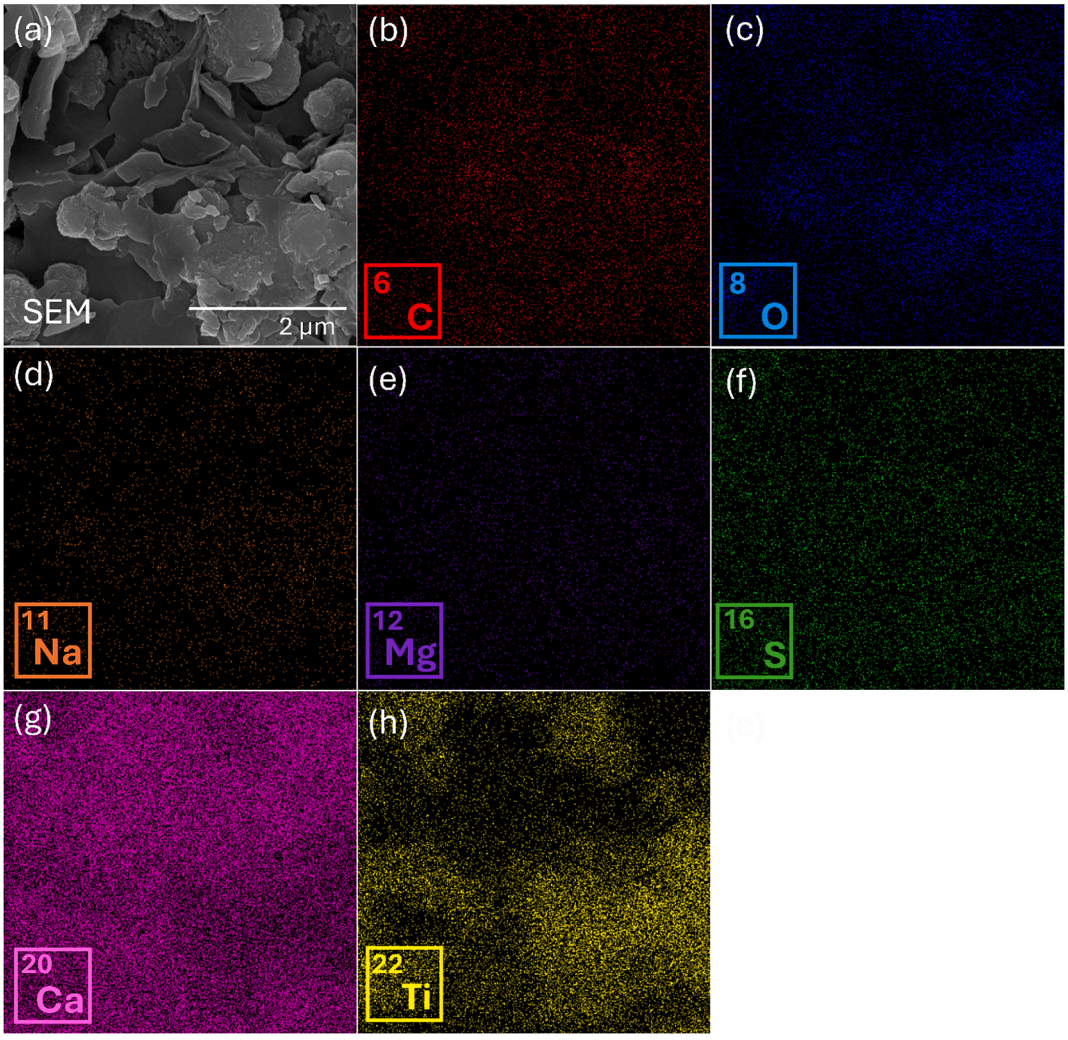

Fig. 9. (a) Representative SEM image of TiO_2 coated limestone substrate, with EDX maps of (b) carbon, (c) oxygen, (d) sodium, (e) magnesium, (f) sulfur, (g) calcium, and (h) titanium.

enhanced photocatalytic activity observed for both pollutants under solar radiation.

The stability of the coatings was evaluated with several photocatalytic cycles, and it can be seen that after the third cycle, a slight deterioration of the photocatalytic activity of the coating was observed (Fig. 8.b). The coated substrate after 3 cycles was observed, and from SEM and EDX analyses (Fig. 9), it is clear that the TiO_2 NP coating persists on the surface of the limestone façade. Residues of MO are also present in the substrate after the cycling experiments, due to the presence of Na and S (Fig. 9. d and Fig. 9. f). The presence of these elements proves that MO residues accumulate after each cycle in the substrate porosity, resulting in decreased photocatalytic efficiency.

From the approach developed in this study, it can be stated that the enhanced specific surface area with the uniform coverage of the substrates impacted the photocatalytic degradation of both RhB and MO pollutant model dyes under solar radiation. Moreover, the combined effects of photocatalytic photodegradation and superhydrophilicity endow the coating with the needed characteristics to be self-cleaning. To the best of the authors' knowledge, this is the first systematic investigation of a microwave synthesised TiO_2 coating at the atomic level. The study demonstrated the coating's adhesion properties to a limestone substrate, its superhydrophilicity without UV exposure, and its enhanced photocatalytic activity under solar radiation, effectively degrading two model dyes while maintaining stability over multiple cycles.

Conclusions

In an innovative approach to enhancing the durability and aesthetics of natural stone façades (limestone), this study reported the development and characterization of self-cleaning coatings using TiO_2 nanoparticles. The high specific surface area microwave synthesised anatase nanoparticles were uniformly deposited on the limestone substrates while preserving the natural appearance of the stone. The self-cleaning properties of the coated substrates were rigorously evaluated through static contact angle measurements and photocatalytic activity tests using rhodamine B and methyl orange as model pollutant dyes. The results were promising, demonstrating a significant increase in hydrophilicity with a near-zero static contact angle, indicating total wettability. Superhydrophilicity is a key characteristic for self-cleaning surfaces, enabling efficient removal of debris and pollutants by rainwater. In the present study, it seems to occur due to a synergetic effect of the nano/micro-structures at the surface and intrinsic properties of the nanomaterial. The TiO_2 coating resisted multiple adhesion cycles, and it demonstrated reusability after consecutive photocatalytic cycling tests under solar radiation, revealing stable performance over time. This is an essential aspect for practical applications, ensuring that the coatings maintain their effectiveness and do not require frequent reapplication. This study provides a sustainable and scalable solution for creating self-cleaning natural stone façades.

CRediT authorship contribution statement

David Henriques Bento: Writing – original draft, Data curation, Conceptualization. **Maria Leonor Matias:** Validation, Data curation, Conceptualization. **Maria Magalhães:** Data curation, Conceptualization. **Catarina Quitério:** Data curation, Conceptualization. **Ana Pimentel:** Validation, Data curation, Conceptualization. **Dora Sousa:** Writing – review & editing, Conceptualization. **Pedro Amaral:** Writing – review & editing. **Carlos Galhano:** Validation. **Elvira Fortunato:** Writing – review & editing, Resources, Project administration. **Rodrigo Martins:** Resources, Project administration. **Daniela Nunes:** Writing – review & editing, Supervision, Investigation.

Funding

This work received support from National Funds from FCT – Fundação para a Ciência e a Tecnologia, I.P., through the project UIDB/50025/2020–2023, UIDP/50025/2020–2023, LA/0037/2020 of the Associate Laboratory Institute of Nanostructures, Nanomodelling, and Nanofabrication-i3N. M.L. Matias would like to express gratitude to FCT for the Ph.D. scholarship UI/BD/151292/2021. Acknowledgments are also extended to the EC projects SYNERGY H2020-WIDESPREAD-2020–5, CSA, proposal n° 952169, and EMERGE-2020-INFRAIA-2020–1, proposal n° 101008701. We are deeply thankful to the Sustainable StonebyPortugal project, proposal number C644943391-00000051 co-financed by the PRR – Recovery and Resilience Plan of the European Union (Next Generation EU).

Declaration of competing interest

The authors declare the following financial interests/personal relationships which may be considered as potential competing interests: Daniela Gomes reports financial support was provided by NOVA University Lisbon NOVA School of Science & Technology. Daniela Gomes reports a relationship with NOVA University Lisbon NOVA School of Science & Technology that includes: employment. If there are other authors, they declare that they have no known competing financial interests or personal relationships that could have appeared to influence the work reported in this pape.

Appendix A. Supplementary data

Supplementary data to this article can be found online at https://doi.org/10.1016/j.clema.2025.100294.

Data availability

Data will be made available on request.

References

Alanazi, T.I., 2023. Current spray-coating approaches to manufacture perovskite solar cells. Results in Physics 44, 106144. https://doi.org/10.1016/j.rinp.2022.106144.

Amano, F., Nogami, K., Tanaka, M., Ohtani, B., 2010. Correlation between Surface Area and Photocatalytic Activity for Acetaldehyde Decomposition over Bismuth Tungstate Particles with a Hierarchical Structure. *Langmuir* 26 (10), 7174–7180. https://doi.org/10.1021/la904274c.

Anandgaonker, P., Kulkarni, G., Gaikwad, S., Rajbhoj, A., 2019. Synthesis of TiO_2 nanoparticles by electrochemical method and their antibacterial application. *Arabian Journal of Chemistry* 12 (8), 1815–1822. https://doi.org/10.1016/j.arabjc.2014.12.015.

Anil Kumar, P.P., 2015. 'Overview of Natural Stones as an Energy Efficient and Climate Responsive Material Choice for. Green Buildings' 27–35. https://doi.org/10.1007/978-3-319-11961-8_3.

Standard Test Methods for Rating Adhesion by Tape Test, Feb. 01, 2023, *ASTM International, ASTM D3359-23, West Conshohocken, PA*. https://doi.org/10.1520/D3359-23.

Balakrishnan, G., Velavan, R., Mujasam Batoo, K., Raslan, E.H., 2020. Microstructure, optical and photocatalytic properties of MgO nanoparticles. Results in Physics 16, 103013. https://doi.org/10.1016/j.rinp.2020.103013.

Barilyuk, D.V., Korol, A.A., Chikanova, E.S., Lomakina, M.A., Shtansky, 2024. Highly hydrophilic TiO_2 nanoparticles as Pickering emulsion stabilizers: synthesis and application. The Journal of Physical Chemistry B 128 (32), 7903–7911. https://doi.org/10.1021/acs.jpcb.4c03315.

Bergamonti, L., et al., 2016. Photocatalytic self-cleaning TiO_2 coatings on carbonatic stones. Applied Physics A: Materials Science & Processing 122 (2), 1–12. https://doi.org/10.1007/S00339-015-9560-Y.

Bolis, V., et al., 2012. Hydrophilic/hydrophobic features of TiO_2 nanoparticles as a function of crystal phase, surface area, and coating, in relation to their potential toxicity in peripheral nervous system. Journal of Colloid and Interface Science 369 (1), 28–39. https://doi.org/10.1016/j.jcis.2011.11.058.

Branquinho, R., Carlos, E., Nunes, D., Fortunato, E., and Martins, R., 'Sustainable Synthesis of Oxides for Electronics and Photocatalysis', in *Synthesis and Applications in Chemistry and Materials*, vol. Volume 14, in Series on Chemistry, Energy and the Environment, vol. Volume 14, WORLD SCIENTIFIC, 2023, pp. 443–482. https://doi.org/10.1142/9789811283239_0043.

Briševac, D., Gabelica, I., Ljubas, D., Bafti, A., Matijašić, G., Ćurković, L., 2024. Effects of TiO_2 Nanoparticles Synthesized via Microwave Assistance on Adsorption and Photocatalytic Degradation of Ciprofloxacin. Molecules 29 (12). https://doi.org/10.3390/molecules29122935.

Calia, A., Lettieri, M., Masieri, M., Pal, S., Licciulli, A., Arima, V., 2017. Limestones coated with photocatalytic TiO_2 to enhance building surface with self-cleaning and depolluting abilities. The Journal of Cleaner Production 165, 1036–1047. https://doi.org/10.1016/j.jclepro.2017.07.193.

Choi, M.-H., Hong, C.-Y., Park, Y.-C., 2024. The hydrophilicity mechanism of anatase and rutile (110) TiO_2 films based on donor-acceptor complexes. *Thin Solid Films* 797, 140349. https://doi.org/10.1016/j.tsf.2024.140349.

Del Secco, B., et al., 2022. Particles Emission from an Industrial Spray Coating Process Using Nano-Materials. Nanomaterials 12 (3). https://doi.org/10.3390/NANO12030313.

Drunka, R., Grabis, J., Krumina, A., 2016. Microwave assisted synthesis, modification with platinum and photocatalytical properties of TiO_2 nanofibers. *Medziagotyra* 22 (1), 138–141. https://doi.org/10.5755/j01.ms.22.1.7353.

Fujishima, A., Zhang, X., 2006. Titanium dioxide photocatalysis: present situation and future approaches. *Comptes Rendus Chimie* 9, 750–760. https://doi.org/10.1016/j.crci.2005.02.055.

Fornasini, L. et al., 2019, 'Photocatalytic N-doped TiO_2 for self-cleaning of limestones', *The European Physical Journal Plus 2019 134:10*, vol. 134, no. 10, pp. 1–13, https://doi.org/10.1140/EPJP/I2019-12981-6.

Gázquez, M. J., Moreno, S. M. P., and Bolívar, J. P., 2021, 'TiO_2 as white pigment and valorization of the waste coming from its production', *Titanium Dioxide (Tio2) and Its Applications*, pp. 311–335, https://doi.org/10.1016/B978-0-12-819960-2.00011-0.

Gryparis, C., Krasoudaki, T., Maravelaki, P.N., 2022. Self-cleaning coatings for the protection of cementitious materials: the effect of carbon dot content on the enhancement of catalytic activity of TiO_2. *Coatings* 12 (5), 587. https://doi.org/10.3390/COATINGS12050587/S1.

Guo, Y., Li, H., Chen, J., Wu, X., Zhou, L., 2014. TiO_2 mesocrystals built of nanocrystals with exposed 001 facets: Facile synthesis and superior photocatalytic ability. Journal of Materials Chemistry A 2 (46), 19589–19593. https://doi.org/10.1039/c4ta05068a.

Gupta, T., Samriti, J.C., Prakash, J., 2021. Hydrothermal synthesis of TiO_2 nanorods: formation chemistry, growth mechanism, and tailoring of surface properties for photocatalytic activities. Materials Today Chemistry 20, 100428. https://doi.org/10.1016/j.mtchem.2021.100428.

Gupta, S., Tripathi, M., 2012. A review on the synthesis of TiO_2 nanoparticles by solution route. Central European Journal of Chemistry. 10 (2), 279–294. https://doi.org/10.2478/s11532-011-0155-y.

Hosono, E., Matsuda, H., Honma, I., Ichihara, M., Zhou, H., 2007. Synthesis of a perpendicular TiO2 nanosheet film with the superhydrophilic property without UV irradiation. *Langmuir* 23 (14), 7447–7450. https://doi.org/10.1021/la701117a.

Kameya, Y., Yabe, H., 2019. Optical and superhydrophilic Characteristics of TiO_2 Coating with Subwavelength Surface Structure Consisting of Spherical Nanoparticle Aggregates. Coatings 9 (9). https://doi.org/10.3390/coatings9090547.

Lettieri, M., Calia, A., Licciulli, A., Marquardt, A.E., Phaneuf, R.J., 2017. Nanostructured TiO_2 for stone coating: assessing compatibility with basic stone's properties and photocatalytic effectiveness. *Bulletin of Engineering Geology and the Environment* 76 (1), 101–114. https://doi.org/10.1007/S10064-015-0820-Z.

Lettieri, M., Colangiuli, D., Masieri, M., Calia, A., 2019. Field performances of nanosized TiO_2 coated limestone for a self-cleaning building surface in an urban environment. Building and Environment 147, 506–516. https://doi.org/10.1016/j.buildenv.2018.10.037.

Lu, L., Zhu, L., Liu, X., Li, J., 2022. Self-cleaning mechanisms and laws of hydrophilic or hydrophobic surfaces of solar photovoltaic glass. *Chemical Engineering Research and Design* 188, 364–377. https://doi.org/10.1016/j.cherd.2022.09.055.

Luttrell, T., Halpegamage, S., Tao, J., Kramer, A., Sutter, E., Batzill, M., 2015. Why is anatase a better photocatalyst than rutile? - Model studies on epitaxial TiO_2 films. Scientific Reports 4. https://doi.org/10.1038/srep04043.

Karapanagiotis, I., and Manoudis, P. N., 2022, 'Superhydrophobic and superamphiphobic materials for the conservation of natural stone: An overview', *Construction and Building Materials*, vol. 320, 126175.https://doi.org/10.1016/j.conbuildmat.2021.126175.

Makuła, P., Pacia, M., Macyk, W., 2018. How To Correctly Determine the Band Gap Energy of Modified Semiconductor Photocatalysts Based on UV-Vis Spectra. The Journal of Physical Chemistry Letters 9. https://doi.org/10.1021/acs.jpclett.8b02892.

Matias, M.L., et al., 2022b. Floating TiO_2-cork nano-photocatalysts for water purification using sunlight. Sustainability (switzerland) 14 (15). https://doi.org/10.3390/su14159645.

Matias, M.L., et al., 2023. Microwave Synthesis of Visible-Light-Activated g-C_3N_4/TiO_2 Photocatalysts. *Nanomaterials* 13 (6), 1090. https://doi.org/10.3390/NANO13061090/S1.

Matias, M.L., et al., 2022a. Enhanced Fe-TiO_2 Solar Photocatalysts on Porous Platforms for Water Purification. Nanomaterials 12 (6). https://doi.org/10.3390/nano12061005.

Mittal, T., 'Nano TiO_2-Based Smart Superhydrophilic Self-Cleaning Surfaces', in Photocatalysts, N. S. Awwad, S. S. Alarfaji, and A. Alomary, Eds., Rijeka: IntechOpen, 2022, ch. 4. https://doi.org/10.5772/intechopen.108157.

Mokrzycki, W., Tatol, M., 2011. Color difference Delta E-A survey Colour difference ΔE-A survey. Machine Graphics and Vision 20 (4), 383–411.

Mousavi, S.H., Silva, A., de Brito, J., Ekhlassi, A., Hosseini, S.B., 2021. Degradation assessment of natural stone claddings over their service life: Comparison between tehran (Iran) and Lisbon (Portugal). *Buildings* 11 (10). https://doi.org/10.3390/buildings11100438.

Nam, C.T., Yang, W.-D., Duc, L.M., 2013. Solvothermal Synthesis of TiO_2 Photocatalysts in Ketone Solvents with Low Boiling Points. Journal of Nanomaterials, 627385. https://doi.org/10.1155/2013/627385.

Nunes, D., et al., 2019, 'Metal oxide nanostructures for sensor applications', *Semiconductor Science and Technology* vol. 34, 043001. https://doi.org/10.1088/1361-6641/ab011e.

Nunes, D., Pimentel, A., Branquinho, R., Fortunato, E., Martins, R., 2021. Metal oxide-based photocatalytic paper: A green alternative for environmental remediation. MDPI. https://doi.org/10.3390/catal11040504.

Padmanabhan, N. T., and John, H., 2020, 'Titanium dioxide based self-cleaning smart surfaces: A short review', *Journal of Environmental Chemical Engineering,* vol. 8, 104211, https://doi.org/10.1016/j.jece.2020.104211.

Pires, V., Rosa, L.G., Amaral, P.M., Dionísio, A., Simão, J.A.R, 2022.. Experimental studies of the effect of SO_2 on the mechanical properties of selected cladding natural stones. Journal of Materials in Civil Engineering 34 (6). https://doi.org/10.1061/(ASCE)MT.1943-5533.0004223.

Quagliarini, E., Bondioli, F., Goffredo, G.B., Cordoni, C., Munafò, P., 2012. Self-cleaning and de-polluting stone surfaces: TiO_2 nanoparticles for limestone. Construction and Building Materials 37, 51–57. https://doi.org/10.1016/j.conbuildmat.2012.07.006.

Rabajczyk, A., Zielecka, M., Klapsa, W., and Dziechciarz, A., 2021, 'Self-Cleaning Coatings and Surfaces of Modern Building Materials for the Removal of Some Air Pollutants', *Materials 2021, Vol. 14, Page 2161*, vol. 14, no. 9, p. 2161, https://doi.org/10.3390/MA14092161.

Raghavan, S., 'TiO_2 Nanostructures by Sol-Gel Processing', in *Sol-Gel Method*, J. P. Singh, S. S. Acharya, S. Kumar, and S. K. Dixit, Eds., Rijeka: IntechOpen, 2023, p. Ch. 3. https://doi.org/10.5772/intechopen.111440.

Rodrigues, A.L., et al., 2019. 'Paleoenvironmental considerations based on geochemistry and mineralogy of a Miocene lacustrine calcrete, southern Portugal', in *E3S Web of Conferences*. EDP Sciences. https://doi.org/10.1051/e3sconf/20199806012.

Rouquerol, J., Llewellyn, P., Rouquerol, F., 2007. 'Is the BET equation applicable to microporous adsorbents? *Studies in Surface Science and Catalysis* 160, 49–56. https://doi.org/10.1016/S0167-2991(07)80008-5.

Rusu, D., Muntean, R., 2022. Using natural stone for buildings - an analysis of educational programs in Romania. IOP Conference Series: Materials Science and Engineering 1242 (1), 012033. https://doi.org/10.1088/1757-899x/1242/1/012033.

Sanchez Tobon, C., Ljubas, D., Mandić, V., Panžić, I., Matijašić, G., Ćurković, L., 2022. Microwave-Assisted Synthesis of N/TiO_2 Nanoparticles for Photocatalysis under Different Irradiation Spectra. Nanomaterials 12 (9). https://doi.org/10.3390/nano12091473.

Rao Kandregula, G., et al., *Green Synthesis of TiO_2 Nanoparticles Using Hibiscus Flower Extract Light Rare Earth/ Lanthanide (Ce & Sm) Oxides decorated on Nano-Carbon for Sensing Applications View project Effects of Temperature, Deposition Time and Catalyst Loading on the Synthesis of Carbon Nanotubes in a Fixed Bed Reactor View project Green Synthesis of TiO_2 Nanoparticles Using Hibiscus Flower Extract*. 2014. [Online]. Available: https://www.researchgate.net/publication/303445315.

Schneider, C. A., Rasband, W. S., and Eliceiri, K. W., 2012, 'NIH Image to ImageJ: 25 years of image analysis', *Nature Methods 2012 9:7*, vol. 9, no. 7, pp. 671–675, https://doi.org/10.1038/nmeth.2089.

Schneider, J., et al., 2014. Understanding TiO_2 photocatalysis: Mechanisms and materials. Chemical Reviews 114. https://doi.org/10.1021/cr5001892.

Shaban, M., Zayed, M., Hamdy, H., 2017. Nanostructured ZnO thin films for self-cleaning applications. RSC Advances 7 (2), 617–631. https://doi.org/10.1039/C6RA24788A.

Silva, T.P., et al., 2022. Contribution to the understanding of the colour change in bluish-grey limestones. Heritage 5 (3), 1479–1503. https://doi.org/10.3390/heritage5030078.

Snethlage, R., 2011. 'Natural stones in architecture: Introduction', in *Stone in Architecture: Properties, Durability*, Springer. Berlin Heidelberg 1–10. https://doi.org/10.1007/978-3-642-14475-2_1.

Spinelli, R., et al., 2019. Development of methodology for determining the physical properties of natural and innovative materials. Advanced Materials Research 1156, 79–96. https://doi.org/10.4028/www.scientific.net/amr.1156.79.

Suwarnkar, M.B., Dhabbe, R.S., Kadam, A.N., Garadkar, K.M., 2014. Enhanced photocatalytic activity of Ag-doped TiO_2 nanoparticles synthesized by a microwave assisted method. Ceramics International 40 (4), 5489–5496. https://doi.org/10.1016/j.ceramint.2013.10.137.

Syafiq, A., et al., 2022. Application of transparent self-cleaning coating for photovoltaic panel: a review. Current Opinion in Chemical Engineering 36, 100801. https://doi.org/10.1016/J.COCHE.2022.100801.

Thommes, M., et al., 2015. Physisorption of gases, with special reference to the evaluation of surface area and pore size distribution (IUPAC Technical Report). *Pure and Applied Chemistry* 87 (9–10), 1051–1069. https://doi.org/10.1515/pac-2014-1117.

Wang, Z., et al., 2020. Preparation and characterization of TiO_2 nanoparticles by two different precipitation methods. Ceramics International 46 (10 Part A), 15333–15341. https://doi.org/10.1016/j.ceramint.2020.03.075.

Wang, J.J., Wang, D.S., Wang, J., Zhao, W.L., Wang, C.W., 2011. High transmittance and superhydrophilicity of porous TiO_2/SiO_2 bi-layer films without UV irradiation. Surface and Coatings Technology 205 (12), 3596–3599. https://doi.org/10.1016/j.surfcoat.2010.12.033.

Wei, X., Zhu, G., Fang, J., Chen, J., 2013. Synthesis, characterization, and photocatalysis of well-dispersible phase-pure anatase TiO_2 nanoparticles. *International Journal of Photoenergy* 2013. https://doi.org/10.1155/2013/726872.

Wu, P., Xue, Z., Yu, T., Penkov, O.V., 2023. Transparent Self-Cleaning Coatings. In: A Review. Multidisciplinary Digital Publishing Institute (MDPI). https://doi.org/10.3390/coatings13071270.

Yang, G., Park, S.J., 2019. Conventional and Microwave Hydrothermal Synthesis and Application of Functional Materials. A Review. Materials 12 (7). https://doi.org/10.3390/MA12071177.

Žerjav, G., Žižek, K., Zavašnik, J., Pintar, A., 2022. Brookite vs. rutile vs. anatase: What's behind their various photocatalytic activities? Journal of Environmental Chemical Engineering 10 (3), 107722. https://doi.org/10.1016/j.jece.2022.107722.

Zhang, J., Zhou, P., Liu, J., Yu, J., 2014. New understanding of the difference of photocatalytic activity among anatase, rutile and brookite TiO_2. *Physical Chemistry Chemical Physics* 16 (38), 20382–20386. https://doi.org/10.1039/c4cp02201g.

Zhou, M., et al., 2021. Aggregation behavior of poly(acrylic acid-co-octadecyl methacrylate) and bovine serum albumin in aqueous solutions. *ChemistryOpen* 10 (3), 373–379. https://doi.org/10.1002/open.202000336.

Zorba, V., Chen, X., Mao, S.S., 2010. Superhydrophilic TiO_2 surface without photocatalytic activation. Applied Physics Letters 96 (9). https://doi.org/10.1063/1.3291667.